Experimental Research on the Impact of Confining Pressure on the Permeability Characteristics of Non-Darcy Flow in Post-failure Rocks

H. Xu, Y. Zhao, W. Bu

Abstract. Researches on the impact of the confining pressure on the permeability characteristics of non-Darcy flow in rocks during the post-failure behaviour plays a significant role in the instability of the non-Darcy flow systems. The permeability characteristics of non-Darcy flow under different confining pressures is studied using a patented device combined with the MTS815.02. The experimental data indicates that the permeability rate of the non-Darcy flow decreases with the increasing in the confining pressure and this relationship can be fitted by an exponential function, while the absolute value of the β factor of non-Darcy flow increases with the increasing in the confining pressure and the relationship can be fitted by a logarithmic function.

Keywords: rock mechanics, post-failure behaviour, non-Darcy flow, confining pressure, permeability, laboratory research.

1. Introduction

The rock matrix can be considered as a porous media showing low permeability under low stress levels and reasonable agreement with the linear relationship of seepage which is also called Darcy law. It was firstly observed on the experiment on the movement of water in pipes (Darcy, 1858). Then, the capillary tube model (Scheidegger, 1953), the network model (or fractured model) (Fatt, 1956; Snow, 1965; Parsons, 1966), the hydraulic radius model (Willie *et al.*, 1952; Carman, 1956), the flow resistance model (Rumer, 1969) and the equation of Navier-Stokes (Whitaker, 1966) were used to obtain the Darcy law in theory. Common permeability tests on rock matrix can get this linear relationship of seepage and are operated on the more intact and denser rocks, while study on the permeability of post-failure rocks has not attracted enough attention so far. In fact, using Darcy law to describe rock permeability in general brings to errors with random permeability rate, no matter that the rocks are in pre-peak stage or post-failure stage (Cheng *et al.*, 2004). According to the practices in mining engineering and the theory of mining pressure and strata control, the stress in surrounding rocks usually exceeds its ultimate strength and the plastic zones are also formed in surrounding rocks. There are many fractures in surrounding rocks. It is called that the surrounding rocks of coal mining are in the state of post-failure. So, the permeability coefficient of surrounding rocks is higher than the permeability coefficient of intact and denser rocks by several orders of magnitude. In addition, the hydraulic pressure in aquifer is higher, sometimes being more than 5 MPa or even more. The water inrush usually occurs in a short time according to the actual disasters in mining engineering. The sudden change in seepage is the primary cause of water inrush disaster, while the linear relationship of seepage can't explain the sudden change in seepage. Thus, it can be concluded that the seepage in surrounding rocks has a nonlinear relationship, which is called non-Darcy flow. In recent years, Professor Xie Xing Miao puts forward the key water-resisting strata theory (Miao *et al.*, 2007; Miao *et al.*, 2008) and seepages instability model (Miao *et al.*, 2004), and establishes rock seepage under mining theory and points out that the destabilization of non-Darcy system in post-failure rocks is the key to water inrush and coal-gas outburst dynamic disasters (Miao *et al.*, 2003), and that has a close relationship with the permeability rate and the β factor of non-Darcy flow. Meanwhile, the coal mining engineering is different from the common underground rock engineering, in which the boundary of mining surrounding rocks is time-varying boundary condition and the confining pressure of post-failure rocks is changing continuously (Ma *et al.*, 2006; Sun *et al.*, 2003). Therefore, it is of great importance to the destabilization of non-Darcy system to carry out some researches on the influence of confining pressure on the permeability characteristics of non-Darcy flow during the post-failure behaviour.

This paper uses a patented device which is combined with the Electro-hydraulic Servo-controlled Rock Mechanics Testing System (which is called MTS815.02) as a new testing system. The experimental scheme and testing system for non-Darcy flow in post-failure rocks are designed. The permeability characteristics of non-Darcy flow in sand shale, limestone and sandstone during the post-

Hui Xu, PhD, Postgraduate, School of Mechanics & Civil Engineering, China University of Mining & Technology, Xuzhou, China. e-mail: xu_hui521@126.com.
Yu Cheng Zhao, Tutor for Doctor, Professor, School of Mechanics & Civil Engineering, China University of Mining & Technology, Xuzhou, China. e-mail: zhaoyc1972@163.com.
Wan Kui Bu, PhD, Associate Professor, Resources and Environment Department, Heze University, Heze, China. e-mail: bwk239@126.com.
Submitted on November 21, 2012; Final Acceptance on June 3, 2015; Discussion open until December 31, 2015.

failure behaviour are obtained with different confining pressure. According to the experimental data, the relationship between the permeability characteristics of non-Darcy flow and confining pressure are analysed and presented for sand shale, limestone and sandstone during the post-failure behaviour. In this paper, the permeability characteristics of non-Darcy flow mainly include two parameters: (1) the permeability rate of non-Darcy flow; (2) the β factor of non-Darcy flow.

2. Experimental Principle and Methodology

The permeability experiments of unconsolidated porous media show that the relationship between pressure gradient ∇p (Pa/m) and seepage velocity $\vec{V}$ (m/s) can be described using the Forchheimer Equation considering the inertia and turbulence effects. Eq. 1 shows the relationship between pressure gradient ∇p and seepage velocity $\vec{V}$ (Forchheimer, 1901; Kong, 1999; Wang *et al.*, 2006):

$$\nabla p = -\frac{\mu}{k}\vec{V} - \rho\beta V\vec{V} \tag{1}$$

In this equation, p is the pressure (Pa), μ is the dynamic viscosity (Pa.s), k is the non-Darcy flow permeability (m^2), ρ is the fluid density (kg/m^3) and β is the β factor of non-Darcy flow (m^{-1}).

The momentum equation of the one-dimensional non-Darcy flow based on Forchheimer relation is showed in Eq. 2.

$$\rho c_a \frac{\partial V}{\partial t} = -\frac{\partial p}{\partial x} - \frac{\mu}{k}V - \rho\beta V^2 + F \tag{2}$$

where C_a is related to the acceleration coefficient of fluid, F is related to the body forces (N) and t is the time (s).

When the time is above to some critical value, the seepage achieves a stable condition and the pressure distribution along the axial rock is a linear function, as shown in Eq. 3 (the fluid compressibility is not considered).

$$\rho p = \left[\frac{\mu}{k}(\rho V) + \beta(\rho V)^2\right](h - x) \tag{3}$$

where h is the height of rock specimen (m), and x is the distance to the bottom of rock specimen (m).

Thus, the pressure gradient can be approximately described by the ratio of pressure difference Δp at the ends of rock specimen and the height of rock specimen h, which is recorded as δp in Eq. 4.

$$\delta p = \frac{\Delta p}{h} = \frac{\mu}{k}V + \rho\beta V^2 \tag{4}$$

In this equation, the permeability rate of non-Darcy flow k and the β factor of non-Darcy flow are used to describe the permeability characteristics. Thus, the pressure (or pressure gradient) and seepage velocity (or mass flow rate) signals are collected to determine the non-Darcy flow permeability characteristics. There are more than ten methods for testing permeability characteristics of rock specimen in laboratory (Miao *et al.*, 2004), but these methods can be roughly divided into two types: stable method and transient method. The stable method tests the stable seepage velocity by keeping the pressure gradient unchanged and gets the permeability characteristics by the fitting curve of pressure gradient and seepage velocity. However, the transient method tests a series of pressure gradient within a certain period of time and calculates the pressure gradient changing rate. Thus, the transient method gets the permeability characteristics by the fitting curve of pressure gradient and pressure gradient changing rate. There are three disadvantages for the transient method: (1) it is difficult to seal the rock specimen; (2) the testing can't keep going on when the pore pressure is greater than the confining pressure; (3) the testing also can't keep going on when the axial strain of rock specimen equals to zero (Wang *et al.*, 2006). Therefore, the stable method is taken to test the permeability characteristics of non-Darcy flow in this paper.

The proposed assemblage (one MTS815.02 coupled with a developed patented device) were used to obtain the relationship between the pressure gradient and the seepage velocity (δp-V). Here, the seepage velocity V is controlled by the velocity of supercharger's piston V_p in MTS815.02. Equation 5 shows the relationship between the seepage velocity V and the velocity of supercharger's piston V_p:

$$V = \frac{d_p^2}{d^2}V_p \tag{5}$$

In this equation, d_p *is* the diameter of the supercharger's piston (m) and d the diameter of the rock specimen (m).

Considering a group of seepage velocity V_1, V_2, ..., V_n and a group of corresponding stable pressure gradients δp_1, δp_2, ..., δp_n, the parameters μ/k and $\rho\beta$ can be obtained by fitting the pressure gradient and the seepage velocity using the second-order polynomial:

$$\frac{\mu}{k} = \frac{\sum_{i=1}^{n}\left.\frac{\partial p}{\partial x}\right|_i V_i(i)\sum_{k=1}^{n}V_k^4(k) - \sum_{i=1}^{n}\left.\frac{\partial p}{\partial x}\right|_i V_i^2(i)\sum_{k=1}^{n}V_k^3(k)}{\sum_{i=1}^{n}V_i^2(i)\sum_{k=1}^{n}V_k^4(k) - \sum_{i=1}^{n}V_i^3(i)\sum_{k=1}^{n}V_k^3(k)} \tag{6}$$

$$\rho\beta = \frac{\sum_{i=1}^{n}\left.\frac{\partial p}{\partial x}\right|_i V_i^2(i)\sum_{k=1}^{n}V_k^2(k) - \sum_{i=1}^{n}\left.\frac{\partial p}{\partial x}\right|_i V_i(i)\sum_{k=1}^{n}V_k^3(k)}{\sum_{i=1}^{n}V_i^2(i)\sum_{k=1}^{n}V_k^4(k) - \sum_{i=1}^{n}V_i^3(i)\sum_{k=1}^{n}V_k^3(k)} \tag{7}$$

Thus, the permeability rate k and the β factor of non-Darcy flow can be obtained by using Eq. 5 to Eq. 7.

For explaining how the permeability rate k and the β factor of non-Darcy flow are obtained, the experimental

data of rock specimen during the post-failure behaviour, taken from the reference (Miao *et al.*, 2004) as an example, are listed in Table 1. During these testing, the dynamic viscosity of fluid μ is 1.01 x 10^{-3} (Pa.s), the fluid density ρ is 1.0 x 10^{3} (kg/m^3) and the diameter of the supercharger's piston d_p is 5.5 x 10^{-2} (m). The permeability rate *k* and the β factor of non-Darcy flow are calculated by combining the equations from Eq. 5 to Eq. 7, which are listed in Table 2.

Table 2 - The permeability characteristics of rock specimen during the post-failure behaviour.

Number of rock specimen	Permeability rate *k* (m^2)	β factor of non-Darcy flow (m^{-1})
1	7.47 x 10^{-15}	1.72 x 10^{15}
2	9.99 x 10^{-15}	1.56 x 10^{15}
3	5.20 x 10^{-15}	1.23 x 10^{15}
4	8.62 x 10^{-15}	1.01 x 10^{15}

3. Experimental System and Scheme

3.1 Experimental system

The experimental system includes a patented device made in China (shown in Fig.1) and MTS815.02 (shown in Fig.2) working together. Heat shrinkable plastic film is used to seal the cylindrical surface of rock specimen. Porous plate (No.4) and felt pad (No.5) are used at the upper end of the rock specimen. The porous plate is designed to make the fluid flow evenly and the felt pad is used to avoid the MTS815.02 System being polluted by the fluid. The rock specimen and the cylinder bore (No.7) are separated by epoxy resin preventing the radial flow. The cylinder bottom of patented device and the pedestal of MTS815.02 are connected by the one-way valve, which including spool (No.11), valve casing (No.12), spring (No.10), baffle (No.13) and bolt (No.9). Standardized sealing ring with "O" type is used to enclose the axial gaps between the cover plate (No.2) and the spherical indenter of axial load system in MTS815.02, the cover plate and the cylinder bore, the cylinder bore and valve casing, and the cylinder bottom of patented device and the pedestal of MTS815.02.

The fluid flows from the pore pressure system in MTS815.02 and goes through globe valves S12 and S14 into the rock specimen, and outflows through porous plates, felt pad and globe valves S1 and S15 in order.

3.2. Experimental scheme

The rock specimen is pressed in post-failure at a given strain value with uniaxial compression in

Table 1 - The experimental data of rock specimen during the post-failure behaviour.

Number of rock specimen	Diameter of rock specimen (m)	Height of rock specimen (m)	The velocity of supercharger's piston (m/s)	Pressure gradient (Pa)
1	5.36 x 10^{-2}	9.21 x 10^{-2}	0.03 x 10^{-3}	0.215 x 10^{6}
			0.05 x 10^{-3}	0.755 x 10^{6}
			0.10 x 10^{-3}	3.11 x 10^{6}
			0.15 x 10^{-3}	6.42 x 10^{6}
			0.20 x 10^{-3}	9.38 x 10^{6}
2	5.34 x 10^{-2}	9.82 x 10^{-2}	0.03 x 10^{-3}	0.455 x 10^{6}
			0.05 x 10^{-3}	0.841 x 10^{6}
			0.10 x 10^{-3}	2.44 x 10^{6}
			0.15 x 10^{-3}	6.01 x 10^{6}
			0.20 x 10^{-3}	8.76 x 10^{6}
3	5.36 x 10^{-2}	9.91 x 10^{-2}	0.03 x 10^{-3}	0.531 x 10^{6}
			0.05 x 10^{-3}	1.23 x 10^{6}
			0.10 x 10^{-3}	3.64 x 10^{6}
			0.15 x 10^{-3}	5.98 x 10^{6}
			0.20 x 10^{-3}	9.45 x 10^{6}
4	5.38 x 10^{-2}	9.86 x 10^{-2}	0.03 x 10^{-3}	0.151 x 10^{6}
			0.05 x 10^{-3}	0.689 x 10^{6}
			0.10 x 10^{-3}	2.43 x 10^{6}
			0.15 x 10^{-3}	4.45 x 10^{6}
			0.20 x 10^{-3}	6.61 x 10^{6}

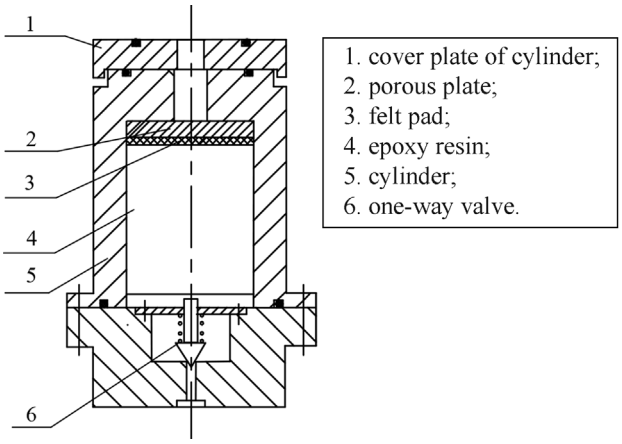

Figure 1 - Patented device in the experimental system.

MTS815.02. Because the axial strain of rock specimen is very small, such as, the maximum axial strain is 0.03 during the testing, the height of rock specimen after unloading can be approximately equal to the height before unloading. In order to prevent the rock pieces emerge from the womb after fracturing, a plastic film is used to seal the cylinder surface and the influence of the plastic film on the rock specimen deformation is tiny.

The assembly is used for steady-state permeability measurement. The confining pressure is fixed at $P_c = 4$ MPa firstly, and then the seepage velocity or pressure are controlled by the pore pressure system. TestStar IIm Controller, including a network distributor, two computers and testing software, is used to collect and process the experimental data. After that, the confining pressure P_c is changed to 6 MPa, 8 MPa, 10 MPa, 14 MPa respectively and then the above-mentioned process should be repeated.

Table 3 - The physical properties of rock samples.

Rock	Density/(gcm^3)	Porosity/(%)	Water absorption/(%)
Sand shale	2.33	1.02	2.33
Limestone	2.62	2.21	0.83
Sandstone	2.51	5.35	5.15

Experimental Results and Analysis

The specimens used in the tests were prepared in sand shale, limestone and sandstone from the Shanxi Province of China. The Physical properties of rock samples are listed in Table 3. The permeability tests were performed under different confining pressure. The fluid was water with density ρ equalling to 1,000 kg/m^3 and dynamic viscosity μ equalling to 1.01 x 10^{-3} Pa.s. The non-Darcy permeability characteristics of the rock specimens (non-Darcy permeability rate k, β factor of non-Darcy flow) could be computed using the data obtained from the tests. The relationship between the confining pressure P_c and the non-Darcy permeability rate k and the relationship between the confining pressure P_c and the β factor of the non-Darcy flow for the three rock types studied are showed in Figure 3a-c.

According to Fig. 3 based on the experimental data, the permeability (k) of the non-Darcy flow for the sand shale, the limestone and the sandstone in post-failure, decrease with the increasing in the confining pressure P_c. The correlation coefficient (Table 4) shows a good fitting with an exponential function. In fact, the confining pressure has restrictive effect on the fracture deformation of transverse tensile, and the increasing of the confining pressure makes the axial fractures to be closed in the specimen. With the

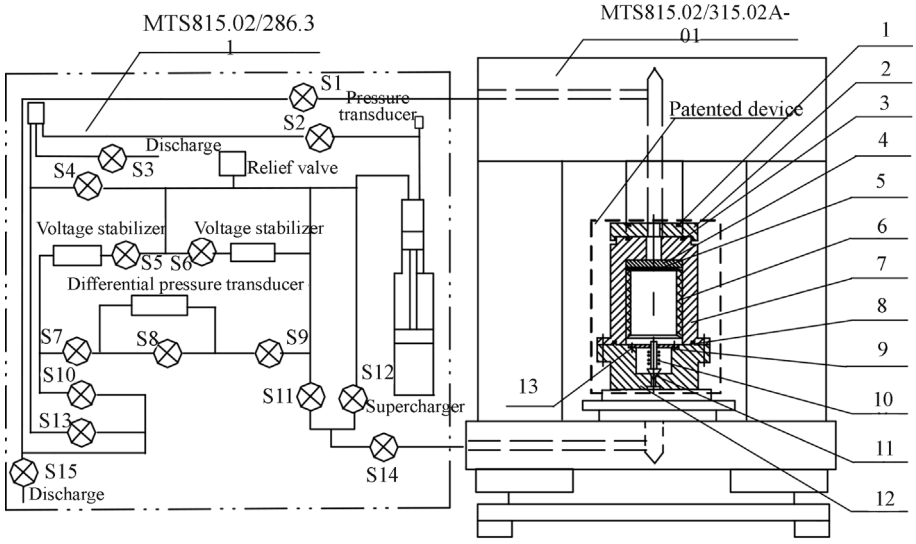

1. nut; 2. cover plate of cylinder; 3. bolt; 4. porous plate; 5. felt pad; 6. epoxy resin; 7. cylinder; 8. nut; 9. bolt; 10. spring; 11. spool; 12. valve casing; 13. baffle.

Figure 2 - Coupled assembly used in the experiment (MTS815.02 with a developed patented device).

Table 4 - Fitting function between non-Darcy permeability k and confining pressure P_c.

Rock	Fitting function	Correlation coefficient
Sand shale in post-failure	$k = 8.66 \times 10^{-19} e^{-0.165Pc}$	0.9586
Limestone in Post-failure	$k = 1.42 \times 10^{-17} e^{-0.126Pc}$	0.9309
Sandstone in Post-failure	$k = 3.84 \times 10^{-17} e^{-0.253Pc}$	0.9472

axial fractures closing, the roughness of the fracture walls and the rock bridges change, affecting the aperture, the tortuosity of the flow channels and the resistance effect on the fluid flow, which also leads to the permeability decreasing. In addition, the permeability of the non-Darcy flow in post-failure rocks is higher than that in intact and denser rocks by one or two orders of magnitude, which can explain the sudden change in seepage in surrounding rocks when the coal seam is excavated.

The absolute values of the β factor of non-Darcy flow for the sand shale, the limestone and the sandstone in post-failure increase with the increasing in the confining pressure as shown in Fig.4a-c. The relationship between the value of the β factor of the non-Darcy flow and the confining pressure P_c can be well fitted by a logarithmic function as shown in Table 5.

4. Conclusion

The rock matrix seepage, especially in post-failure state, which is a main factor for the water inrush disasters in geotechnical engineering (Galybin, 1997; Wu *et al.*, 2004; Nomikos *et al.*, 2011), shows the characteristics of

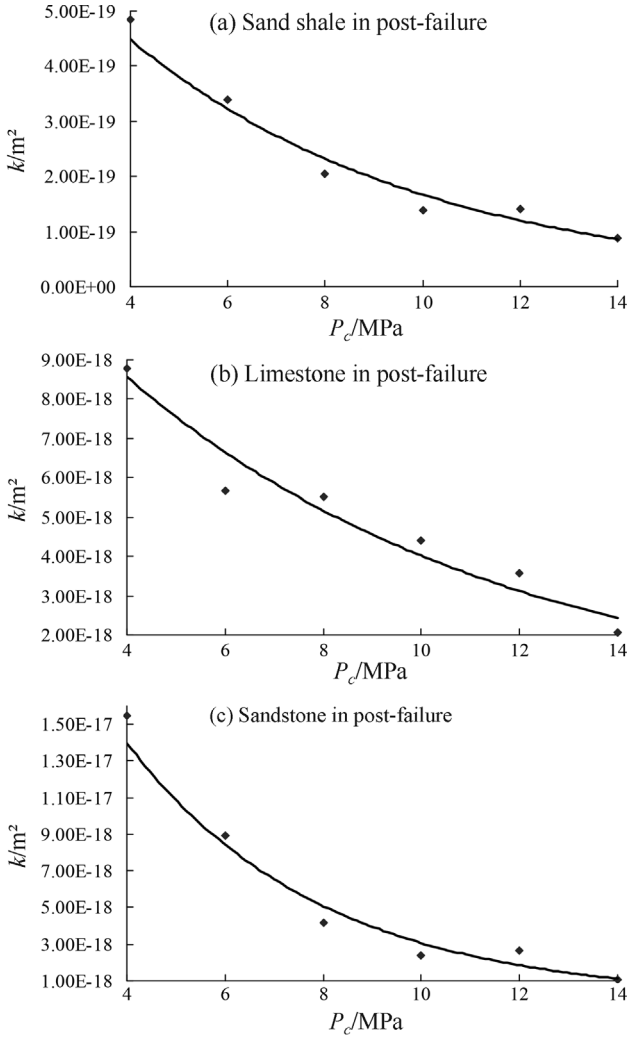

Figure 3 - Relationship between the non-Darcy permeability (k) and the confining pressure (P_c) for the three rock types.

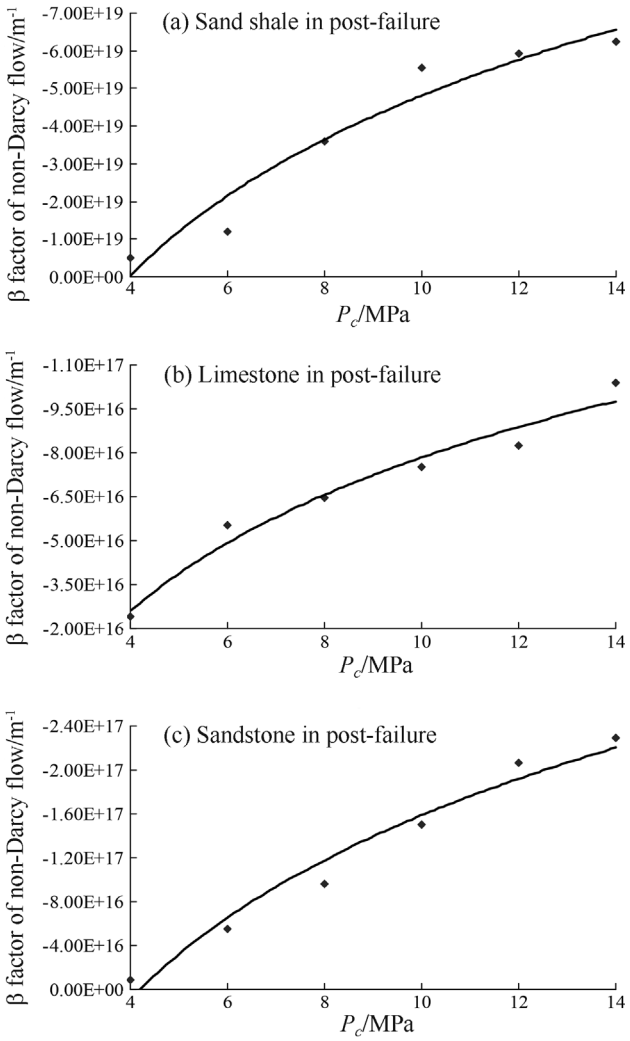

Figure 4 - Relationship between the β factor of the non-Darcy flow and the confining pressure (P_c) for the three rock types.

Table 5 - Fitting functions between the value of β factor of non-Darcy flow and confining pressure P_c.

Rock	Fitting function	Correlation coefficient
Sand shale in post-failure	$\beta = -(5.22\ln(P_c)+7.20) \times 10^{19}$	0.9432
Limestone in Post-failure	$\beta = -(5.71\ \ln(P_c)+5.32) \times 10^{16}$	0.9647
Sandstone in Post-failure	$\beta = -(1.83\ \ln(P_c)+2.62) \times 10^{17}$	0.9663

non-Darcy flow. In this paper the combined assemblage of a patented device with MTS815.02 were used to study the non-Darcy flow permeability in three rock types considering different confining pressures. The experimental data show that the permeability rate of the non-Darcy flow decreases with the increasing of the confining pressure and the best fit is achieved through an exponential function. Also, the absolute value of the β factor of the non-Darcy flow increases with the increasing of the confining pressure and the best fit is achieved through a logarithmic function. The experimental data show that the permeability of the non-Darcy flow in post-failure rocks is higher than that in intact and denser rocks by one or two orders of magnitude. So, it can be concluded that the non-Darcy flow in post-failure rocks is one of the main factors for the water inrush disasters in rock engineering. Thus, these experimental data and related expressions in this paper will provide an important basis for the seepage destabilization in the layered rocks.

Acknowledgments

Financial support for this work, provided by the National Basic Research Program of China (973 Program) (No.2007CB209400), the Key Project of National Nature Science Foundation of China (No.50834004), the China Postdoctoral Science Foundation (No.20110491486) and the Research Foundation of Heze University(No.XY14KJ01) are gratefully acknowledged.

References

Carman, P.C. (1956). Flow of Gases Through Porous Media. Butterworths Scientific Publications, London, 182 p.

Cheng, Y.K.; Chen, Z.Q.; Miao, X.X. & Mao, X.B. (2004). Testing study on permeability of non-Darcy flow in post-peak sandstone. Chinese Journal of Rock Mechanics and Engineering, 23(12):2005-2009 (in Chinese).

Darcy, H.P.G. (1858). Experimental research on the movement of water in pipes. Mémoires Présentés à l'Académie des Sciences de l'Institut de France, 14:141 (in French).

Fatt, I. (1956). The network model of porous media. Trans Am Inst Mem Metall Pet Eng, 207:144-181.

Forchheimer, P.Z. (1901). Wasserbewegungdurch Boden. Zeitschrift des Vereins Deutscher Ingenieure, 45:1782-1788.

Galybin, A.N. (1997). A model of mining-induced fault sliding. International Journal of Rock Mechanics and Mining Sciences. 34(3-4):91-103.

Kong, X.Y. (1999). Advanced Percolation Mechanics. University of Science and Technology of China Press, Hefei, pp. 55-63 (in Chinese).

Ma, Z.G.; Huang, W.; Guo, G.L. & Chen, Z.Q. (2006). Analysis on failure of covering rock in ehuobulake mine by using mechanics of systems with variable boundaries. Journal of Liaoning Technical University, 25(4):515-517 (in Chinese).

Miao, X.X.; Chen, R.H. & Bai, H.B. (2007). Fundamental concepts and mechanical analysis of water-resisting key strata in water-preserved mining. Journal of China Coal Society, 32(6):561-564 (in Chinese).

Miao, X.X.; Chen, Z.Q.; Mao, X.B. & Chen, R.H. (2003). The bifurcation of non-Darcy flow in post-failure rock. Acta Mechanica Sinica, 35(6):660-667 (in Chinese).

Miao, X.X.; Liu, W.Q. & Chen, Z.Q. (2004). Dynamics of Systems of Seepage Flow in Surrounding Rock Affected by Mining. Science Press, Beijing, pp 33-49 (in Chinese).

Miao, X.X.; Pu, H. & Bai, H.B. (2008). Principle of water-resisting key strata and its application in water-preserved mining. Journal of China University of Mining & Technology, 37(1):1-4 (in Chinese).

Nomikos P.P. & Sofianos A.I. (2011) An analytical probability distribution for the factor of safety in underground rock mechanics. International Journal of Rock Mechanics and Mining Sciences, 48(4):597-605.

Parsons, R.W. (1966). Permeability of idealized fractured rock. Society of Petroleum Engineers Journal, 6(2):126-136.

Rumer, R.R. (1969). Resistance to flow through porous media, Flow through Porous Media, Academic Press, New York, pp. 91-108.

Scheidegger, A.E. (1953). Theoretical models of porous matter. Producers Monthly, 17(10):17-23.

Snow, D.T. (1965). A Parallel Plate Model of Fractured Permeable Media. Ph.D. Thesis, Department of Civil Engineering, University of California, Berkeley, 331 p.

Sun, M.G.; Tang, P. & Chen, Z.Q. (2003). Expectation on dynamic system with variable boundary. Journal of Changde Teachers University (Natural Science Edition), 15(2):12-15 (in Chinese).

Wang, X.S. & Chen, Z.Q. (2006). Hydrodynamic analysis of transient method in rock seepage tests. Chinese Jour-

nal of Rock Mechanics and Engineering, 25(S1):3098-3103 (in Chinese).

Whitaker, S. (1966). The equations of motion in porous media. Chemical Engineering Science, 21(3):291-300.

Wu, Q.; Wang, M. & Wu, X. (2004). Investigations of groundwater bursting into coal mine seam floors from fault zones. International Journal of Rock Mechanics and Mining Sciences, 41:557-571.

Wyllie, M.R. & Spangler, M.B. (1952). Application of electrical resistivity measurements to problem of fluid flow in porous media. Bulletin of the American Association of Petroleum Geologists, 36(2):359-403.